Effect of Underpotentially Deposited Adlayers on Sulfur Bonding Schemes of Organothiols Self-Assembled on Polycrystalline Gold: sp or sp^3 Hybridization

I-Wen Peter Chen, Chien-Chieh Chen, Shu-Yi Lin, and Chun-hsien Chen*

Department of Chemistry, National Tsing Hua University, Hsinchu, Taiwan 30013, R.O C.

Received: June 10, 2004; In Final Form: August 26, 2004

Improvement in stability of self-assembled monolayers (SAMs) has been demonstrated by using an underpotentially deposited (upd) interlayer between the SAMs and gold substrate. In this study, we show that the upd adlayers can be applied to improve the packing density of thiophenol SAMs due to controlling the binding scheme of the sulfur headgroup from an sp^3 to an sp hybridization configuration. Examined here are the structures of SAMs on gold substrate pre-modified by four types of upd adatoms that are electrodeposited at several coverages representing the finish of distinct upd processes. The SAM structures of a homologous series of *n*-alkanethiols ($CH_3(CH_2)_nSH$, $n = 4-11$ and $13-15$) are characterized by contact angle measurements and infrared reflectance absorption spectroscopy. The results show the odd−even effect that the orientation of the terminal methyl group is alternatively associated with the number of methylene units, indicating that sulfur headgroup adopts an sp^3 hybridization on Au/Bi(upd) and an sp hybridization on Au/Ag(upd) and Au/Cu(upd). For SAMs on Au/Hg(upd) at a low upd coverage, an sp^3 hybridization of the sulfur headgroup is in favor of short chain alkanethiols. As the number of methylene unit increases, the molecular axis appears to align toward the surface normal, suggesting that intermolecular attractions become more influential than the sulfur bonding scheme on the SAM structures on Au/Hg(upd). In contrast, at a high upd coverage of Au/Hg(upd), the sulfur headgroup adopts an sp hybridization as indicated by the odd−even characteristics. In all cases, the increase in the coverage of upd adatoms results in a smaller tilt angle of the molecular axis with respect to the surface normal.

Introduction

Organothiol self-assembled monolayers (SAMs) have attracted enormous research interests during the last two decades[1−5] and will continue to do so in the future because of the ease in assembly, the excellent properties as model systems, and their fascinating applications at the molecular level, such as sensors,[6−8] catalysis,[9] microlithography, and molecular electronics.[10] For applications at elevated temperature,[11−13] requiring long-term exposure to liquid media,[14] or involving further fabrication of molecular architecture on preexisting SAMs,[15−20] major concerns are film integrity and structural order, resulting from the interplay between intermolecular and sulfur headgroup−substrate interactions. To strengthen the stability of SAMs, the methods to reinforce intermolecular interactions include integrating aromatic moieties in the adsorbate molecules,[21−24] introducing intermolecular hydrogen bonding,[12,25−30] and polymerization within SAMs;[31−36] the strategies to improve the headgroup−substrate interactions include the use of adsorbates that can potentially form multiple headgroup−substrate bonds[21,37,38] and pre-modification of gold substrate with a monatomic interlayer by underpotential deposition (upd).[39−48]

In principle, the selection of substrate that interacts strongly with the molecular headgroup can improve the stability of organosulfur SAMs against desorption under harsh experimental conditions. Numerous studies point out that the sulfur headgroup adsorbs more strongly[49−55] and exhibits better stability[55−57] on silver and copper than on gold. Nevertheless, gold is the most favorable substrate for thiol-based SAMs because the advantage of chemical inertness grants the excellent reproducibility in preparing high-quality monolayers, whereas silver and copper develop active surface oxides that readily attract ubiquitously carbonaceous contaminants and makes difficult the formation of densely packed SAMs. Jennings and Laibinis[39,40] initiated an alternative that effectively improves the thermal stability of SAMs by upd of Ag or Cu monolayers on the Au surface prior to assembly of SAMs. Upd,[58−61] first reported by Rogers in 1949,[62,63] is an electrochemical process that a submonolayer or full monolayer of foreign metal atoms can be electrodeposited at a potential positive of the reversible Nernst potential of its bulk form because of stronger adatom−substrate interactions than those between adatoms. Upd has been ascribed to a result of a larger work function of the substrate than that of the adatom.[58−61] Measurements by X-ray photoelectron spectroscopy reveal a larger binding energy of the upd interlayer than its bulk form, no indication of oxides on Au/Ag(upd), and only a slight amount of oxides found on Au/Cu(upd),[40−44] suggesting that the upd adlayer exhibits electron deficiency. During the course of SAM preparation under ambient conditions, the electron deficiency suppresses the formation of surface oxides and provides a better reproducibility of SAMs than those on the corresponding bulk material.[47] With the intriguing properties, the upd adatoms enhance significantly the thermal[39,40,47] and electrochemical stability[41,64,65] of SAMs, regardless of whether the upd interlayer is electrodeposited prior to[41] or following[64,65] the SAM assembly. The upd adlayers have been shown to promote headgroup−substrate anchoring and assembly of alkanephosphonate,[48] alkanoic acids,[42,47] and pyrrole[43,44] mono-

* To whom correspondence should be addressed. Phone: (+886) 3-573-7009. Fax: (+886) 3-571-1082. E-mail: chhchen@mx.nthu.edu.tw.

10.1021/jp047495p CCC: $27.50
Published on Web 10/14/2004

layers that would otherwise exhibit no chemisorption on bare gold. Furthermore, it has been demonstrated that the stability and electric conductivity of electropolymerized polypyrrole is substantially improved by the upd interlayer.[43,44]

Stability of SAMs can be reinforced by intermolecular attractions or by a high degree of monolayer crystallinity, a balance of the interplay between intermolecular and headgroup−substrate interactions. A remarkable example to elucidate the interplay is thioaromatic SAMs ($X-(C_6H_4)_m-(CH_2)_n-SH$, $X = H$, CH_3, NO_2, etc.), whose packing density is dependent on the numbers of the phenyl ring and methylene unit.[5,66,67] It is generally agreed that bonding of the sulfur headgroup on gold preferentially adopts an sp^3 hybridization with an Au−S−C bond angle of ∼104°.[23,68−70] This bonding geometry dictates the structure of thiophenol ($m = 1$, $n = 0$) monolayers. The bond angle imposes steric constrains that diminish intermolecular attractions between neighboring phenyl rings and result in poorly defined monolayers.[5,22,23,70−75] With the increasing number of rings ($m \geq 2$, $n = 0$), the monolayer becomes either more densely packed or well ordered, attributable to the shift of the dominant factor from headgroup−substrate interactions to intermolecular attractions.[5,22,23,76] The steric constrains can be released by inserting an odd number of methylene unit between the aryl and the sulfur headgroup. For an odd number of methylene unit, the thioaromatic SAMs are more densely packed and exhibit smaller tilt angles than those having even methylene units.[66,77,78] The opposite is true on a silver substrate[68,79] where the preferable bonding scheme for the sulfur headgroup is an sp hybridization with an Ag−S−C bond angle of ∼180°.[68,75,80] This example also manifests that high crystallinity and thus stability of SAMs can be achieved by manipulating the headgroup−substrate interactions, an alternative to synthesizing or purchasing molecules with the desired structure.

Electrodeposition of upd adlayers modifies surface properties and provides a means to manipulate the sulfur−substrate bonding configuration. The spacing between upd adatoms can be controlled to some extent, and therefore, the monolayer packing structure may be adjusted. The bonding scheme of sulfur headgroup on upd-modified gold is important, yet unexplored. Herein, we examine SAMs on polycrystalline gold pre-electrodeposited by Ag, Cu, Hg (in sulfuric acid), and Bi (in perchloric acid) upd, which exhibit distinct open adlattice structures prior to bulk deposition. At low upd coverages, stable structures of Ag, Cu, Hg, and Bi upd on Au(111) are (3×3), $(\sqrt{3}\times\sqrt{3})R30°$, $(\sqrt{3}\times\sqrt{19})$, and (2×2), respectively.[61,81,82] As electrode potentials are potentiostated negatively, the coverage of upd adatoms increases and eventually upd adatoms become close-packed. Upon assembly of alkanethiol monolayers, the various degrees of open spaces present within the upd-modified gold surface may provide an avenue to fine-tune the intermolecular distance, packing density, and the molecular tilt angle with respect to the surface normal. In this study, the upd-modified substrates are prepared at various adatom coverages whose effect on the SAM structures is investigated. The structure of a homologous series of *n*-alkanethiol SAMs is characterized by contact angle measurements and infrared reflectance absorption spectroscopy (IRAS). The hybridization scheme of the sulfur headgroup is investigated by systematically examining the orientation of the terminal methyl group. The results show that the sulfur headgroup adopts an sp^3 hybridization on Au/Bi(upd) and an sp hybridization on Au/Ag(upd) and Au/Cu(upd). For SAMs on Au/Hg(upd) at a low upd coverage, an sp^3 hybridization of the sulfur headgroup is in favor of short chain alkanethiols. As the methylene units increase, the molecular axis appears to align toward the surface normal, suggesting that intermolecular attractions become more influential than the sulfur bonding scheme for the SAM structures on Au/Hg(upd). On the other hand, an sp hybridization of the sulfur headgroup is found for SAMs on Au/Hg(upd) at a full adlayer coverage.

Experimental Section

Preparation of SAMs on UPD-Modified Gold Surface. Substrates were 200 nm thick gold films thermally evaporated onto glass slides pre-cleaned with piranha solution which is a 1:3 (v/v) mixture of 30% H_2O_2 and concentrated H_2SO_4. ***Caution!*** *This solution reacts violently with organic materials and should be handled with great care*. The pressure in the bell-jar evaporator (Auto 306, Edwards High Vacuum International, West Sussex, U.K.) was nominally 2×10^{-6} Torr. A 10 nm Cr underlayer was used to enhance the adhesion of the gold film. Prior to vapor deposition, the glass slides were preheated at 150 °C in vacuo to thoroughly remove the trace amount of moisture. The gold substrate exhibited domains of flat terraces, as revealed by scanning tunneling microscopy (NanoScope IIIa, Veeco Metrology Group, Santa Barbara, CA). A roughness factor of 1.4 ± 0.2 ($n = 15$) was derived by experiments of Pb upd with 1 mM $Pb(NO_3)_2$ in a solution of 0.10 M $NaClO_4$ and 0.10 M $HClO_4$.[83] The gold films were essentially polycrystalline but with characteristic Au(111) features, probably due to the thermal annealing at 150 °C during vapor deposition.[84]

The upd solutions were prepared from reagent grade chemicals and Millipore-Q purified water (18 MΩ cm^{-1}). The solutions were 0.1 M H_2SO_4 containing 0.6 mM Ag_2SO_4 (Fisher Scientific), 1 mM $CuSO_4$ (May & Baker), and 1 mM HgO (Lancaster), respectively, for Ag, Cu, and Hg upd. Due to ill solubility of Bi_2O_3 in H_2SO_4, 1 mM Bi_2O_3 (Aldrich) was prepared in 0.1 M $HClO_4$ for Bi upd. Because of the large size of the gold substrates (1 in. × 3 in.), a 200 mL beaker was used to hold the electrolytes. The reference electrode for Ag upd was a high-purity silver wire flame-annealed with a butane microtorch and quenched into pure water prior to upd experimentation. A high purity copper wire (Aldrich) was utilized as the reference electrode for Cu upd and was cleaned by dipping into diluted nitric acid (Fisher Scientific) for a short period of time prior to each use. The potentials of the Ag and the Cu wires were 408 ± 2 and 36 ± 2 mV, respectively, against a commercially available Ag/AgCl reference electrode (model MF 2052, BioAnalytical System, West Lafayette, IN) in their corresponding upd solutions used here. The Ag/AgCl was used for upd of Hg and Bi. All potentials reported in the text were referred to $E_{Ag/AgCl}$. Electrochemical experiments were carried out with a CHI 421 (CH Instruments, Austin, TX) or a bipotentiostat (model AFCBP1, Pine Instrument, Grove City, PA). Typical cyclic voltammograms of these upd systems were shown in Figure 1, analogous to literature reports.[61]

Respective initial potentials for Ag, Cu, Hg, and Bi upd were 600 mV (vs $E_{Ag^{+/0}}$), 423 mV, 1015 mV, and 575 mV (vs $E_{Ag/AgCl}$). The substrates were modified by holding the potentials at 460, 250, 100, and 46 mV for Ag upd (vs $E_{Ag^{+/0}}$), 108 and 8 mV for Cu upd, 887 and 527 mV for Hg upd, and 220, 100, and 24 mV for Bi upd (vs $E_{Ag/AgCl}$). The upd modified substrates were subsequently removed under potential control, rinsed with copious ethanol, blown dry in a stream of nitrogen, and transferred rapidly through air into ethanol solutions containing organosulfur molecules.[39−44,46−48,85] The *n*-alkanethiols ($CH_3-(CH_2)_nSH$, $n = 4-11$ and 13−15, Aldrich or TCI) and thiophenol (C_6H_5SH, TCI) were used as received. Soaking solutions

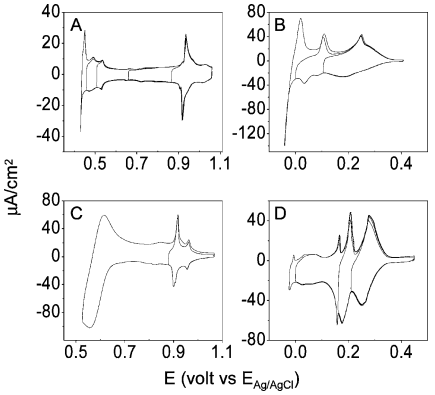

Figure 1. Cyclic voltammograms of (A) Ag, (B) Cu, (C) Hg, and (D) Bi upd on thermally evaporated gold films. The supporting electrolytes are 0.1 M H_2SO_4 for Ag, Cu, Hg upd and 0.1 M $HClO_4$ for Bi upd. The scan rate is 20 mV/s. Voltammograms of Cu, Hg, and Bi upd are obtained in N_2-saturated solutions. The switching potentials are described in the Experimental Section.

were 1 mM of the organosulfurs prepared in ethanol (TEDIA). All substrates were kept in the solution for at least 12 h and then were rinsed thoroughly three times in sequence with ethanol and water and blown dry with nitrogen.

Characterization of SAMs. Wetting measurements were conducted with a contact angle measuring system (FTA-200 goniometer, First Ten Angstroms, Portsmouth, VA) equipped with a digital camera and an analyzing software (FTA Video Drop Shape Analysis Version 1.98). Advancing contact angles were measured on static drops of water or *n*-hexadecane while the needle tip of the syringe remained in the drop. Absorption spectroscopy was carried out with a Perkin-Elmer System 2000 infrared spectrometer equipped with an MCT detector cooled with liquid nitrogen. The measurement scheme was a single reflection mode and the *p*-polarized light was incident at 85° from the surface normal with a grazing angle accessory (FT-85, Spectra-Tech, Shelton, CT). The light path, detector, and sample chambers were purged with dry nitrogen. A total of 1024 scans of both the sample and the reference (bare Au) were collected at 4-cm^{-1} resolution for signal averaging.

Desorption experiments[23,86,87] of thiophenol SAMs to estimate the coverage were performed by attaching the films to an O-ring sidearm of a three-compartment cell. The electrode area was calculated from the reduction charge of gold oxide (386 μC/cm^2).[88] The solution was 0.5 M KOH (Aldrich, semiconductor grade). Nitrogen gas was purged to deaerate for at least 30 min and the nitrogen flow above the solution was maintained during voltammetry.

Results and Discussion

Cyclic Voltammetry and Contact Angle Measurements. Figure 1 shows typical cyclic voltammograms (CVs) for upd of Ag, Cu, Hg in 0.1 M H_2SO_4 and Bi in 0.1 M $HClO_4$. The deposition and stripping peaks are more distinct than those of upd on polycrystalline gold but are not as well defined as peaks on Au(111),[61,82,89,90] indicating that the substrates were preferentially (111)-oriented but polycrystalline in nature. The negative limits of the voltammograms represent the initial stage of the second adlayer[91] or overpotential deposition. The switching potentials in Figure 1 correspond to the finish of distinct upd processes and indicate where the electrodes were removed from upd solutions under potential control and were subsequently subjected to rinsing and immersion into thiol-containing ethanol under open circuit potential. For example, Figure 1A illustrates

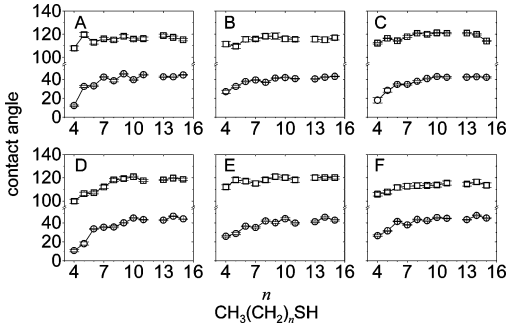

Figure 2. Advancing contact angles for *n*-alkanethiol SAMs on (A) bulk gold, (B) Au/Ag(upd, 868 mV), (C) Au/Ag(upd, 658 mV), (D) Au/Ag(upd, 508 mV), (E) Au/Ag(upd, 454 mV), and (F) bulk silver. The potentials denoted in the parentheses indicate where the electrodes are removed from the upd solution against $E_{Ag/AgCl}$. The probe liquids are water (square) and hexadecane (circle).

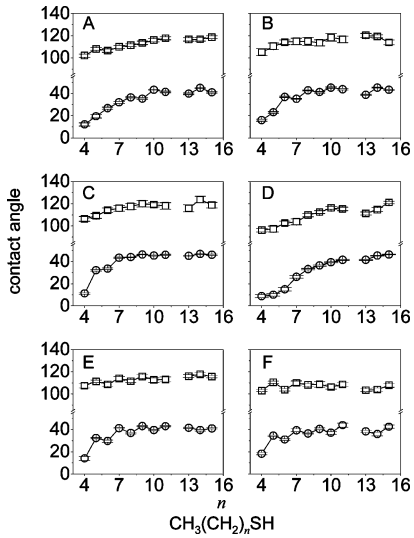

Figure 3. Advancing contact angles for *n*-alkanethiol SAMs on (A) Au/Cu(upd, 108 mV), (B) Au/Cu(upd, 8 mV), (C) Au/Hg(upd, 887 mV), (D) Au/Hg(upd, 527 mV), (E) Au/Bi(upd, 220 mV), and (F) Au/Bi(upd, 24 mV). The probe liquids are water (square) and hexadecane (circle).

that the coverages of Ag adatoms are regulated at upd potentials of 868, 658, 508, and 454 mV versus $E_{Ag/AgCl}$ (equivalent to 460, 250, 100, and 46 mV against $E_{Ag^{+/0}}$) and the wetting behaviors of the *n*-alkanethiol monolayers assembled on the corresponding upd-modified substrates are shown in Figure 2B−E, respectively. For comparison, also presented in Figure 2A,F are monolayers assembled on freshly prepared gold and silver films, respectively. For the cases of Cu, Hg, and Bi upd, the potentials to prepare different upd coverages (namely, at potentials where the electrodes were emerged from electrodeposition solutions) are described in the Experimental Section and the results of contact angle measurements for the subsequent *n*-alkanethiol SAMs are shown in Figure 3.

It is well-known that the upd adlattices for Ag, Cu, and Hg upd are significantly influenced by coadsorption of solution anions.[61] The upd structure and adatom coverage can be manipulated by preparing the upd adlayer in the solution containing desired anions. Sulfate (or bisulfate) adsorbs stronger than most anionic electrolytes and thus their upd CVs in sulfuric acid are more reproducible than any other electrolytes. To minimize the complexity of this study, sulfuric acid is employed for Ag, Cu, and Hg upd. Perchloric acid is arbitrarily used for Bi upd whose CVs and the (2×2) open lattice are independent

of the supporting electrolyte[92] due to the electrostatic repulsion of partial charge remaining on the Bi adatoms.

We measure the contact angles of water and hexadecane (HD) to qualitatively evaluate the degree of order at the methyl terminated SAMs. The uncertainty of sample-to-sample variation is within ±1°. The contact angle increases with *n* (the number of methylene unit) and reaches a limiting value, comparable to that of SAMs prepared on bare gold. In most cases for $n \geq 6$, the water and HD contact angles are larger than 110° and 40°, respectively. The hydrophobicity and oleophobicity indicate a low free-energy surface, generally considered a densely packed and high-quality monolayer.

Due to the high surface tension and the intercalation processes of HD, the contact angle of HD is highly sensitive to small differences in the interfacial structure of alkanethiol SAMs.[93,94] The contact angles of HD on Au/Ag(upd, 454 mV)/SAMs (Figure 2E) show an odd−even effect where the monolayers with an odd number of methylene chains exhibit slightly smaller contact angles than the even ones do. Because interfacial methylene chains are more wettable than interfacial methyl termini, the smaller contact angles for SAMs with an odd *n* suggest a larger tilt for the methyl group such that the probe liquid is more accessible to the methylene groups than those with an even *n*. Consequently, the odd−even effect suggests an Ag−S−C bond angle of 180° and an sp hybridization for the sulfur headgroup on Au/Ag(upd, 454 mV). The HD contact angles of Figure 3A,B (Cu upd) for relative long alkanethiols show an odd−even effect similar to that of Figure 2E, whereas the trend for Figure 3E,F (Bi upd) is the reverse. The results indicate that the sulfur headgroup adopts an sp and an sp^3 hybridization on Au/Cu(upd) and Au/Bi(upd), respectively. For Au/Hg(upd)/SAMs (Figure 3C,D), the contact angle measurements appear to have no odd−even effect and thus the sulfur bonding scheme is inconclusive.

Infrared Reflectance Absorption Spectroscopy (IRAS): General Features. For the convenience of discussion, Au/Ag(upd, 658 mV) is arbitrarily chosen as the substrate for presenting IRAS spectra of $CH_3(CH_2)_nSH$ ($n = 4-11, 13-15$) SAMs (Figure 4). IRAS spectra of SAMs assembled on the other upd-modified substrates are provided in the Supporting Information. As described in detail elsewhere, the vibrational modes at around 2965, 2938, 2918, 2897, and 2850 cm^{-1} are assigned to $\nu_a(CH_3$, ip), $\nu_s(CH_3$, FR), $\nu_a(CH_2)$, $\nu_s(CH_3)$, and $\nu_s(CH_2)$, respectively.[95−99] In all cases, the intensities of $\nu_a(CH_2)$ and $\nu_s(CH_2)$ stretching modes increase with *n*. The peak position of $\nu_a(CH_2)$ generally shifts from 2922 ($n = 7$) to 2918 ($n \geq 11$) cm^{-1}, indicating that the straight alkyl chains form a close-packed and largely *all-trans* assembly.[95−99] The band intensities of $\nu_a(CH_3$, ip) and $\nu_s(CH_3)$ alternate with increasing *n*, confirming the odd−even effect indicated by HD contact angles. The odd−even effect is also evident for other type of upd adatoms and potentials (vide infra).

Effect of upd on Sulfur Bonding Configuration. The IRAS spectra in Figure 4 show an odd−even effect that the intensities of the methyl modes alternate with increasing *n* for alkanethiol SAMs on Au/Ag(upd, 658 mV). IRAS spectra for alkanethiol SAMs prepared on Au/Cu(upd), Au/Hg(upd), and Au/Bi(upd) all exhibit the odd−even effect to some degree. The odd−even dependence of the terminal methyl orientation confirms an *all-trans* conformational arrangement for the methylene chains. The spectra are available in the Supporting Information. Other general features in the series of spectra include the increase in $\nu_{sym}(CH_2)$ and $\nu_{asy}(CH_2)$ peak intensities, and the shift of $\nu_{asy}(CH_2)$ peak position toward 2918 cm^{-1}, suggesting the improvement in film crystallinity associated with increasing number of methylene units.

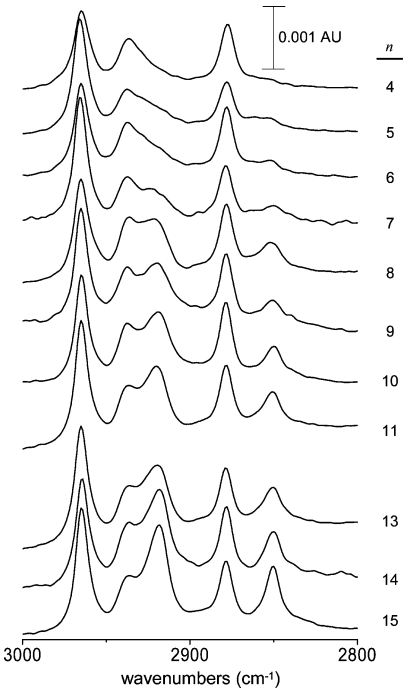

Figure 4. Grazing incidence polarized infrared spectra of $CH_3(CH_2)_nSH$ SAMs on Au/Ag(upd, 658 mV).

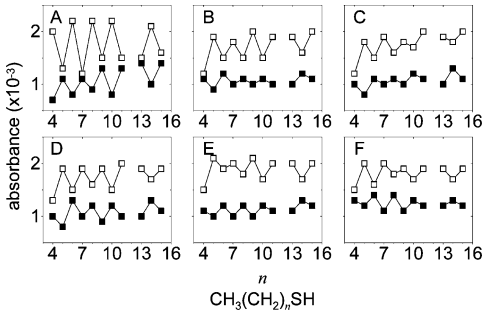

Figure 5. Absorbance of $\nu_a(CH_3$, ip) and $\nu_s(CH_3)$ versus the number of methylene units for SAMs of *n*-alkanethiols on (A) bulk gold, (B) Au/Ag(upd, 868 mV), (C) Au/Ag(upd, 658 mV), (D) Au/Ag(upd, 508 mV), (E) Au/Ag(upd, 454 mV), and (F) bulk silver.

Figures 5 and 6 summarize the odd−even dependence of the methyl stretching bands for *n*-alkanethiol SAMs prepared on a upd-modified gold surface. For comparison, the odd−even effects observed on bare gold and bulk silver are provided in parts A and F of Figure 5, respectively. For alkanethiol SAMs on Au/Ag(upd) (Figure 5B−E) and Au/Cu(upd) (Figure 6A,B), the higher absorbance arises for the odd number of chains with $\nu_{asy}(CH_3$, ip) at 2965 cm^{-1} and with $\nu_s(CH_3)$ at 2878 cm^{-1} for the even-number ones. Such an alternation is the same as those of alkanethiol SAMs on bulk Ag and Cu.[98,99] The bonding configuration of sulfur on substrate modified by Ag upd and Cu upd should be similar to those on bulk Ag and Cu and thus is described as an sp hybridization.[68,75,80] In the case of Au/Bi(upd), the sulfur headgroup should adopt an sp^3 hybridization because the odd−even alternation (Figure 6E,F) is the same as that found on bare gold. Interestingly, the sulfur bonding schemes on Au/Hg(upd) appear dependent on the coverage of Hg adatoms. Figure 6C is obtained at low Hg coverage (Au/Hg(upd, 887 mV)) where a study by in-situ X-ray diffraction identified an open structure of ($\sqrt{3}$x$\sqrt{19}$) adlattice formed by bisulfate stabilized Hg_2^{2+} dimers.[100] The modulation in methyl

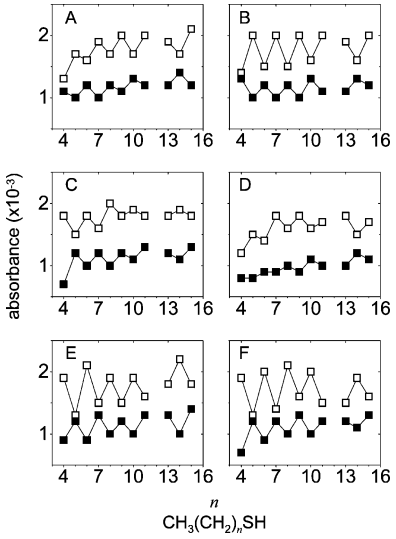

Figure 6. Absorbance of $\nu_a(CH_3$, ip) and $\nu_s(CH_3$, FR) versus the number of methylene units for SAMs of *n*-alkanethiols on (A) Au/Cu(upd, 108 mV), (B) Au/Cu(upd, 8 mV), (C) Au/Hg(upd, 887 mV), (D) Au/Hg(upd, 527 mV), (E) Au/Bi(upd, 220 mV), and (F) Au/Bi(upd, 24 mV). The open and solid squares denote intensities of $\nu_a(CH_3$, ip) and $\nu_s(CH_3)$, respectively.

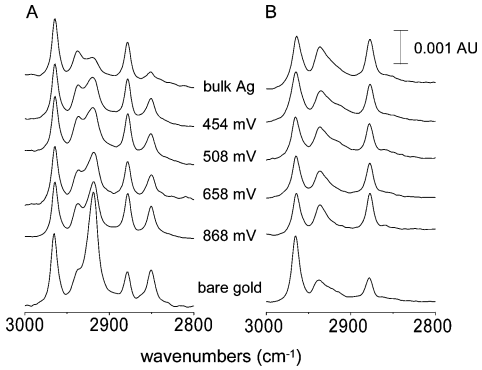

Figure 7. Grazing incidence polarized infrared spectra of (A) $CH_3(CH_2)_{14}SH$ and (B) $CH_3(CH_2)_4SH$ SAMs to illustrate the effect of upd adlayers on short and long-chain alkanethiols, respectively. The substrates are freshly evaporated gold, silver, and Au/Ag(upd) modified at the indicated potentials (vs $E_{Ag/AgCl}$).

stretching is consistent with an sp^3 hybridization bonding scheme for sulfur atoms. The odd−even effect is more pronounced for short thiols than for long ones, suggesting a larger chain-tilt angle for short alkanethiol thiols. On a full monolayer coverage of Hg adatoms, alkanethiol SAMs exhibit an odd−even effect (Figure 6D) opposite to that at low Hg coverage, indicative of an sp hybridization for sulfur bonding on Au/Hg(upd). Although the magnitude of the alternating intensity in methyl stretching is smallest among the upd systems studied here, this instance of Hg upd demonstrates that manipulation of SAM structures via the headgroup bonding scheme is feasible by controlling upd coverage.

Effect of upd Potentials on Chain-Tilt Angles: Long-Chain Thiols. Figure 7 displays IR spectra of *n*-pentadecanethiol ($n = 14$) and *n*-pentanethiol ($n = 4$) SAMs on Au/Ag(upd) as a function of upd potentials that fine-tune the upd coverage and structure of the Ag interlayer. The two alkanethiols represent molecules with long and short methylene chains, corresponding to SAMs with relatively strong and weak intermolecular attractions, respectively. For comparison, spectra of SAMs on bulk gold and silver are also provided. For *n*-pentadecanethiol SAMs (Figure 7A), the intensities of $\nu_a(CH_2)$ and $\nu_s(CH_2)$ are

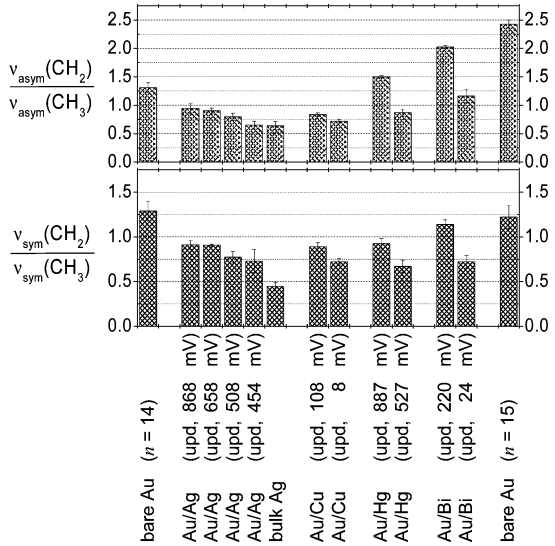

Figure 8. Plot of dichroic ratios of (A) $A_{\nu_{asy}(CH_2)}/A_{\nu_{asy}(CH_3)}$ and (B) $A_{\nu_{sym}(CH_2)}/A_{\nu_{sym}(CH_3)}$ measured for *n*-hexadecanethiol SAMs ($n = 15$).

strongest on gold, smallest on bulk silver, and intermediate for those on Au/Ag(upd). A slight difference between the spectral profiles is noticed between those prepared at different Ag-upd potentials. For example, as the potential for preparing Au/Ag(upd) is potentiostated negatively from 868 mV (namely, increasing the coverage of Ag adatoms from 33% to ca. 100%) the intensity ratios of methylene to methyl stretches for $A_{\nu_{asy}(CH_2)}/A_{\nu_{asy}(CH_3)}$ and $A_{\nu_{sym}(CH_2)}/A_{\nu_{sym}(CH_3)}$ decrease gradually from 0.92 to 0.68 and from 0.71 to 0.58, respectively. Ulman et al.[101] have illustrated that the intensity ratio reflects the level of the alkyl chain tilt angle relative to the surface normal with a smaller ratio attributed to a smaller tilt angle. Therefore, the decrease in the intensity ratio associated with increasing upd coverage shows the effect of Ag upd adlayers on reducing the alkyl chain tilt angle.

To explore the effect of upd adlayers on the alkyl chain tilt, the ratios of $A_{\nu_{asy}(CH_2)}/A_{\nu_{asy}(CH_3)}$ and $A_{\nu_{sym}(CH_2)}/A_{\nu_{sym}(CH_3)}$ for *n*-hexadecanethiol SAMs are summarized in Figure 8. The ratios measured on bare gold and bulk silver are provided to facilitate the comparison. For the cases of Au/Ag(upd) and Au/Cu(upd), *n*-pentadecanethiol, one methylene unit less than *n*-hexadecanethiol, is used on bare gold to compensate for the different hybridization schemes of the sulfur headgroup, whereas, for Au/Bi(upd), the ratios for hexadecanethiol SAMs on bare gold are shown in the right of Figure 8. The results exhibit a general trend of a progressively more vertical orientation for the molecular axis as the coverage of upd adatoms increases. Although we are not able to quantitatively derive the tilt angle due to the limitations of IRAS and film-to-film variation, the estimated values should lie between those of *n*-alkanethiols on gold (20−40°)[96,97,99,102,103] and silver (6−15°).[98,99,104]

Effect of Ag upd Potentials on Chain-Tilt Angles: Short-Chain Thiols. For short alkanethiol SAMs with only a few methylene units, the intensity of $\nu_{asy}(CH_2)$ is too weak to calculate the ratios of methylene to methyl stretches, and thus it is difficult to compare the relative alkyl chain tilt angles (see, for example, Figure 7B). An alternative to explore the effect of upd coverage on the orientation of short alkanethiols is monitoring the evolution of $A_{\nu_{sym}(CH_3)}/A_{\nu_{asy}(CH_3)}$ as a function of upd potentials. The relative tilted angle of the terminal methyl group (not the molecular axis) can be inferred by making use of the *surface dipole selection rule*[1,105] in which only vibrational modes with transition dipole moments aligned perpendicular

to the metal substrate can interact with the IR beam and appear in the IRAS spectra, whereas those aligned parallel with the substrate are missing. A descendant trend in $A_{\nu_{sym}(CH_3)}/A_{\nu_{asy}(CH_3)}$ indicates that the projections of transition dipoles onto the surface normal are gradually diminishing for $\nu_{sym}(CH_3)$ and growing for $\nu_{asy}(CH_3)$; namely, a smaller $A_{\nu_{sym}(CH_3)}/A_{\nu_{asy}(CH_3)}$ indicates a relatively larger tile angle for the methyl group. For example, upon increasing the coverage of Ag adatoms, the $A_{\nu_{sym}(CH_3)}/A_{\nu_{asy}(CH_3)}$ ratios for pentanethiol (Figure 7B) and hexanethiol (Supporting Information) SAMs exhibit a falling trend from 0.94 to 0.70 and a rising trend from 0.35 to 0.47, respectively. The opposite trends suggest that the methyl groups of pentanethiol ($n = 4$, even) and hexanethiol ($n = 5$, odd) SAMs are, respectively, tilting away and pointing toward the surface normal. Given the facts that the sulfur atom adopts an sp hybridization binding scheme on Au/Ag(upd) and that the tilt angle should be smaller than alkanethiol SAMs on gold ($\leq 30°$), the opposite tilting directions for the terminal methyl group demonstrate that increasing the coverage of Ag adatoms exerts an effect of reducing the tilt angle of the molecular axis with respect to the surface normal.

The relative alkyl chain tilt angles between long and short chain thiols can also be qualitatively judged by the alternating magnitudes of $A_{\nu_{sym}(CH_3)}/A_{\nu_{asy}(CH_3)}$ ratio between successive even and odd *n*. Because the $A_{\nu_{sym}(CH_3)}/A_{\nu_{asy}(CH_3)}$ ratio is a function of the orientation of the methyl group, a smaller oscillation in the magnitude indicates a smaller change in the methyl orientation with respect to the surface normal and thus a smaller tilt angle for the molecular axis. Accordingly, in the case of pentanethiol and hexanethiol assembled on Au/Ag(upd), the increase in the coverage of Ag adatoms results in the aforementioned opposite trends that reduce the difference between their $A_{\nu_{sym}(CH_3)}/A_{\nu_{asy}(CH_3)}$ ratios and imply a more upright orientation for the molecular axis. In the case of long-chain thiols, the ratios of $A_{\nu_{sym}(CH_3)}/A_{\nu_{asy}(CH_3)}$ for pentadecanethiol and hexadecanethiol SAMs (Supporting Information) range from 0.77 to 0.72 and 0.55 to 0.60, respectively, upon increasing the coverage of Ag upd adatoms. The difference of $A_{\nu_{sym}(CH_3)}/A_{\nu_{asy}(CH_3)}$ between successive *n* is smaller than that of the short thiols, indicative of a smaller chain tilt angle in general. To sum up, for short thiol SAMs prepared on Au/Ag(upd) at a lower coverage of Ag adatoms, the molecular axis exhibits a larger tilt angle that is probably a result of thiols residing on microscopically rugged substrate developed by the open spacing of the Ag adlayer. The fact that the molecular axes for long alkanethiols are aligned closer to the surface normal and are less affected by Ag upd coverage should be attributed to the increasingly important factor of interchain van der Waals attractions.

Increasing Coverage of Thiophenol SAMs by upd Modification. To demonstrate that the effect of the upd adlayer on the sulfur−substrate binding configuration and, thus, the improvement in film quality, linear sweep voltammetry (LSV) is utilized to estimate the coverage of thiophenol (TP) SAMs on unmodified and upd-modified gold. The phenyl ring of TP on gold is known to be tilted relative to the surface normal,[23,68−70] a result of the sp^3 hybridization of the sulfur atom and the ∼104° angle of Au−S−C. Au/Cu(upd) is not used for comparison because the hydrogen evolution reaction takes place at film defects prior to thiol desorption and thus LSV shows no electrodesorption peaks.[54,64] A typical electroreductive wave of TP from unmodified gold is displayed as the dotted curve in Figure 9. The peak potential is ca. −0.88 V and the charge under the desorptive peak is 40.3 ± 1.0 μC/cm^2. Assuming a one-electron reduction process for thiol desorption,[87] the packing

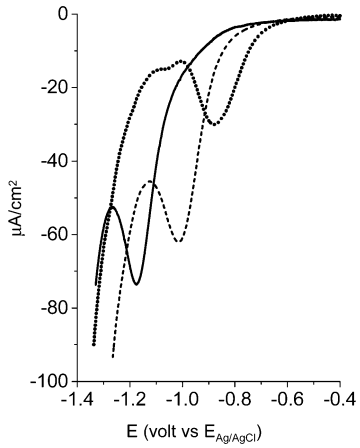

Figure 9. Linear sweep voltammograms for the desoprtion of thiophenol SAMs on bare gold (dotted line), Au/Ag(upd, 658 mV) (dashed line), and Au/Ag(upd, 454 mV) (solid line). The sweep rate was 100 mV/s and the solution was 0.5 M KOH, deaerated by sparging N_2(g) for at least 30 min.

density of TP on unmodified gold is 4.2 × 10^{-10} mol/cm^2. For comparison, the molecular area for a ($\sqrt{3}$x$\sqrt{3}$)R30° lattice on Au(111) is 21.6 Å^2, equivalent to 7.7 × 10^{-10} mol/cm^2 or 74 μC/cm^2. The shape of voltammograms and the coverage are in good agreement with literature reports.[23,74,106]

Typical electrodesorption waves of TP from Au/Ag(upd, 658 mV) and Au/Ag(upd, 454 mV) are shown, respectively, as the dashed and solid curves (Figure 9) where the corresponding peak potentials shift negatively to −1.02 and −1.18 V. The shift in peak potential is attributed to improvement in intermolecular attractions[45,54,87] and to the difference in sulfur−substrate interactions.[45,54,64,65] On both Au/Ag(upd) substrates, the desorption charge is raised to 69.4 ± 3.6 μC/cm^2 (or 7.2 × 10^{-10} mol/cm^2), demonstrating a significant increase in packing density of TP due to a good control of the sulfur binding scheme via the upd adlayer. Yoneyama and co-workers[65] underpotentially electrodeposited Ag on Au pre-assembled with octadecanthiol (OT) SAMs. STM shows that the upd adlayer formed Ag islands at defect sites and the reductive desorption wave of OT SAMs exhibits two well-separated peaks at −1.07 and −1.34 V that are almost identical to that of OT SAMs on Au and Ag surfaces, respectively. In Figure 9, there is only one desorptive peak, indicative of homogeneous distribution of Ag adatoms after TP self-assembly.

Conclusion

In this study we have demonstrated that the structures of *n*-alkanethiol SAMs can be manipulated by pre-deposition of a upd adlayer on gold substrate. Upd of Ag, Cu, Hg, and Bi on gold is examined because their CVs show multiple pairs of deposition−desorption peaks and the adlattices on single crystalline gold exhibit open structures where the nearest neighboring spacing is tunable electrochemically. Contact angle and IRAS measurements unveil an odd−even effect for *n*-alkanethiol SAMs on upd-modified gold, indicative of close-packed and primarily an all-trans configuration of the methylene chain. The odd−even effect shows the sulfur headgroup adopts an sp^3 hybridization on Au/Bi(upd) and an sp hybridization on Au/Ag(upd) and Au/Cu(upd). For SAMs on Au/Hg(upd) at a low upd coverage, an sp^3 hybridization of the sulfur headgroup is favorable for short chain alkanethiols. As the number of methylene units increases, the tilt angle from the surface normal is diminishing and the odd−even effect is less significant,

suggesting that intermolecular attractions become a more influential factor than the effect of the Au/Hg(upd) adlattice on the SAM structures. In contrast, at a high upd coverage of Au/Hg(upd), an sp hybridization of the sulfur headgroup is confirmed by IRAS measurements. In all cases, for short thiol SAMs prepared at a lower coverage of upd adatoms, the molecular axis exhibits a larger tilt angle. Although long alkanethiols show a similar trend, the tilt angle is relatively small and less affected by the upd coverage. The discrepancy between short and long thiols should be attributed to the difference in their interchain van der Waals attractions.

Acknowledgment. We thank the National Science Council (R.O.C.) for financial and research support. S.-Y.L. acknowledges a postdoctoral fellowship from the National Science Council.

Supporting Information Available: IRAS spectra of n-$CH_3(CH_2)_nSH$ ($n = 5-11$, $13-15$) SAMs on Au/Ag(upd), Au/Cu(upd), Au/Hg(upd), and Au/Bi(upd) are available free of charge via the Internet at http://pubs.acs.org.

References and Notes

(1) Ulman, A. *An Introduction to Ultrathin Organic Films: From Langmuir−Blodgett to Self-Assembly*; Academic Press: Boston, 1991.
(2) Ulman, A. *Chem. Rev.* **1996**, *96*, 1533−1554.
(3) Xia, Y.; Rogers, J. A.; Paul, K. E.; Whitesides, G. M. *Chem. Rev.* **1999**, *99*, 1823−1848.
(4) Schreiber, F. *Prog. Surf. Sci.* **2000**, *65*, 151−256.
(5) Yang, G.; Liu, G.-y. *J. Phys. Chem. B* **2003**, *107*, 8746−8759.
(6) Flink, S.; van Veggel, F. C. J. M.; Reinhoudt, D. N. *Adv. Mater.* **2000**, *12*, 1315−1328.
(7) Chaki, N. K.; Vijayamohanan, K. *Biosens. Bioelectron.* **2002**, *17*, 1−12.
(8) Mirsky, V. M. *Trends Anal. Chem.* **2002**, *21*, 439−450.
(9) Kakkar, A. K. *Chem. Rev.* **2002**, *102*, 3579−3588.
(10) Fendler, J. H. *Chem. Mater.* **2001**, *13*, 3196−3210.
(11) Bensebaa, F.; Ellis, T. H.; Badia, A.; Lennox, R. B. *Langmuir* **1998**, *14*, 2361−2367.
(12) Tam-Chang, S.-W.; Biebuyck, H. A.; Whitesides, G. M.; Jeon, N.; Nuzzo, R. G. *Langmuir* **1995**, *11*, 4371−4382.
(13) Delamarche, E.; Michel, B.; Kang, H.; Gerber, Ch. *Langmuir* **1994**, *10*, 4103−4108.
(14) Flynn, N. T.; Tran, T. N. T.; Cima, M. J.; Langer, R. *Langmuir* **2003**, *19*, 10909−10915.
(15) Weckenmann, U.; Mittler, S.; Kramer, S.; Aliganga, A. K. A.; Fischer, R. A. *Chem. Mater.* **2004**, *16*, 621−628.
(16) Lee, J. K.; Lee, K.-B.; Kim, D. J.; Choi, I. S. *Langmuir* **2003**, *19*, 8141−8143.
(17) Hutt, D. A.; Leggett, G. J. *Langmuir* **1997**, *13*, 2740−2748.
(18) Yan, L.; Marzolin, C.; Terfort, A.; Whitesides, G. M. *Langmuir* **1997**, *13*, 6704−6712.
(19) Kwon, Y.; Mrksich, M. *J. Am. Chem. Soc.* **2001**, *124*, 806−812.
(20) Cecchet, F.; Pilling, M.; Hevesi, L.; Schergna, S.; Wong, J. K. Y.; Clarkson, G. J.; Leigh, D. A.; Rudolf, P. *J. Phys. Chem. B* **2003**, *107*, 10863−10872.
(21) Garg, N.; Carrasquillo-Molina, E.; Lee, T. R. *Langmuir* **2002**, *18*, 2717−2726.
(22) Sabatani, E.; Cohen-Boulakia, J.; Bruening, M.; Rubinstein, I. *Langmuir* **1993**, *9*, 2974−2981.
(23) Tao, Y.-T.; Wu, C.-C.; Eu, J.-Y.; Lin, W.-L.; Wu, K.-C.; Chen, C.-h. *Langmuir* **1997**, *13*, 4018−4023.
(24) Ishida, T.; Mizutani, W.; Choi, N.; Akiba, U.; Fujihira, M.; Tokumoto, H. *J. Phys. Chem. B* **2000**, *104*, 11680−11688.
(25) Clegg, R. S.; Hutchison, J. E. *Langmuir* **1996**, *12*, 5239−5243.
(26) Clegg, R. S.; Reed, S. M.; Hutchison, J. E. *J. Am. Chem. Soc.* **1998**, *120*, 2486−2487.
(27) Clegg, R. S.; Hutchison, J. E. *J. Am. Chem. Soc.* **1999**, *121*, 5319−5327.
(28) Clegg, R. S.; Reed, S. M.; Smith, R. K.; Barron, B. L.; Rear, J. A.; Hutchison, J. E. *Langmuir* **1999**, *15*, 8876−8883.
(29) Lewis, P. A.; Smith, R. K.; Kelly, K. F.; Bumm, L. A.; Reed, S. M.; Clegg, R. S.; Gunderson, J. D.; Hutchison, J. E.; Weiss, P. S. *J. Phys. Chem. B* **2001**, *105*, 10630−10636.
(30) Valiokas, R.; Ostblom, M.; Svedhem, S.; Svensson, S. C. T.; Liedberg, B. *J. Phys. Chem. B* **2002**, *106*, 10401−10409.
(31) Willicut, R. J.; McCarley, R. L. *J. Am. Chem. Soc.* **1994**, *116*, 10823−10824.
(32) Willicut, R. J.; McCarley, R. L. *Langmuir* **1995**, *11*, 296−301.
(33) Sayre, C. N.; Collard, D. M. *Langmuir* **1995**, *11*, 302−306.
(34) Ford, J. F.; Vickers, T. J.; Mann, C. K.; Schlenoff, J. B. *Langmuir* **1996**, *12*, 1944−1946.
(35) Kim, T.; Chan, K. C.; Crooks, R. M. *J. Am. Chem. Soc.* **1997**, *119*, 189−193.
(36) Cai, M.; Mowery, M. D.; Menzel, H.; Evans, C. E. *Langmuir* **1999**, *15*, 1215−1222.
(37) Shon, Y.-S.; Lee, T. R. *J. Phys. Chem. B* **2000**, *104*, 8192−8200.
(38) Shon, Y.-S.; Lee, T. R. *Langmuir* **1999**, *15*, 1136−1140.
(39) Jennings, G. K.; Laibinis, P. E. *Langmuir* **1996**, *12*, 6173−6175.
(40) Jennings, G. K.; Laibinis, P. E. *J. Am. Chem. Soc.* **1997**, *119*, 5208−5214.
(41) Zamborini, F. P.; Campbell, J. K.; Crooks, R. M. *Langmuir* **1998**, *14*, 640−647.
(42) Lin, S.-Y.; Tsai, T.-K.; Lin, C.-M.; Chen, C.-h.; Chan, Y.-C.; Chen, H.-W. *Langmuir* **2002**, *18*, 5473−5478.
(43) Liu, Y.-C. *Langmuir* **2003**, *19*, 6888−6893.
(44) Liu, Y.-C.; Chuang, T. C. *J. Phys. Chem. B* **2003**, *107*, 9802−9807.
(45) Fonticelli, M.; Azzaroni, O.; Benitez, G.; Martins, M. E.; Carro, P.; Salvarezza, R. C. *J. Phys. Chem. B* **2004**, *108*, 1898−1905.
(46) Hsieh, M.-H.; Chen, C.-h. *Langmuir* **2000**, *16*, 1729−1733.
(47) Lin, S.-Y.; Chen, C.-h.; Chan, Y.-C.; Lin, C.-M.; Chen, H.-W. *J. Phys. Chem. B* **2001**, *105*, 4951−4955.
(48) Baker, M. V.; Jennings, G. K.; Laibinis, P. E. *Langmuir* **2000**, *16*, 3288−3293.
(49) Hatchett, D. W.; Stevenson, K. J.; Lacy, W. B.; Harris, J. M.; White, H. S. *J. Am. Chem. Soc.* **1997**, *119*, 6596−6606.
(50) Azzaroni, O.; Vela, M. E.; Andreasen, G.; Carro, P.; Salvarezza, R. C. *J. Phys. Chem. B* **2002**, *106*, 12267−12273.
(51) Wang, M.-C.; Liao, J.-D.; Weng, C.-C.; Klauser, R.; Shaporenko, A.; Grunze, M.; Zharnikov, M. *Langmuir* **2003**, *19*, 9774−9780.
(52) Liao, J.-D.; Wang, M.-C.; Weng, C.-C.; Klauser, R.; Frey, S.; Zharnikov, M.; Grunze, M. *J. Phys. Chem. B* **2002**, *106*, 77−84.
(53) Wang, M.-C.; Liao, J.-D.; Weng, C.-C.; Klauser, R.; Frey, S.; Zharnikov, M.; Grunze, M. *J. Phys. Chem. B* **2002**, *106*, 6220−6226.
(54) Azzaroni, O.; Vela, M. E.; Fonticelli, M.; Benitez, G.; Carro, P.; Blum, B.; Salvarezza, R. C. *J. Phys. Chem. B* **2003**, *107*, 13446−13454.
(55) Brewer, N. J.; Foster, T. T.; Leggett, G. J.; Alexander, M. R.; McAlpine, E. *J. Phys. Chem. B* **2004**, *108*, 4723−4728.
(56) Schoenfisch, M. H.; Pemberton, J. E. *J. Am. Chem. Soc.* **1998**, *120*, 4502−4513.
(57) Hutt, D. A.; Cooper, E.; Leggett, G. J. *J. Phys. Chem. B* **1998**, *102*, 174−184.
(58) Kolb, D. M., Gerischer, H., Tobias, C. W., Eds. *Advances in Electrochemistry and Electrochemical Engineering*; Wiley-Interscience: New York, 1978; Vol. 11, pp 125−271.
(59) Adzic, R., Gerischer, H., Tobias, C. W., Eds. *Advances in Electrochemistry and Electrochemical Engineering*; Wiley-Interscience: New York, 1984; Vol. 13, pp 159−260.
(60) Trasatti, S. In *The Work Function in Electrochemistry*; Gerischer, H., Tobias, C. W., Eds.; Advances in Electrochemistry and Electrochemical Engineering; Wiley-Interscience: New York, 1977; Vol. 10, pp 213−321.
(61) Herrero, E.; Buller, L. J.; Abruna, H. D. *Chem. Rev.* **2001**, *101*, 1897−1930 and references therein.
(62) Rogers, L. B. In *Electrochemistry, Past and Present*; Stock, J. T., Orna, M. V., Eds.; ACS Symposium Series No. 390; American Chemical Society: Washington, DC, 1989; pp 396−401.
(63) Rogers, L. B.; Krause, D. P.; Griess, J. C., Jr.; Ehrlinger, D. B. *J. Electrochem. Soc.* **1949**, *95*, 33−46.
(64) Nishizawa, M.; Sunagawa, T.; Yoneyama, H. *Langmuir* **1997**, *13*, 5215−5217.
(65) Oyamatsu, D.; Nishizawa, M.; Kuwabata, S.; Yoneyama, H. *Langmuir* **1998**, *14*, 3298−3302.
(66) Azzam, W.; Cyganik, P.; Witte, G.; Buck, M.; Woll, Ch. *Langmuir* **2003**, *19*, 8262−8270.
(67) Cyganik, P.; Buck, M.; Azzam, W.; Woll, Ch. *J. Phys. Chem. B* **2004**, *108*, 4989−4996.
(68) Sellers, H.; Ulman, A.; Shnidman, Y.; Eilers, J. E. *J. Am. Chem. Soc.* **1993**, *115*, 9389−9401.
(69) Jung, H. H.; Won, Y. D.; Shin, S.; Kim, K. *Langmuir* **1999**, *15*, 1147−1154.
(70) Szafranski, C. A.; Tanner, W.; Laibinis, P. E.; Garrell, R. L. *Langmuir* **1998**, *14*, 3570−3579.
(71) Dhirani, A.-A.; Zehner, R. W.; Hsung, R. P.; Guyot-Sionnest, P.; Sita, L. R. *J. Am. Chem. Soc.* **1996**, *118*, 3319−3320.
(72) Frey, S.; Stadler, V.; Heister, K.; Eck, W.; Zharnikov, M.; Grunze, M.; Zeysing, B.; Terfort, A. *Langmuir* **2001**, *17*, 2408−2415.
(73) Nielsen, J. U.; Esplandiu, M. J.; Kolb, D. M. *Langmuir* **2001**, *17*, 3454−3459.

(74) Zhong, C.-J.; Brush, R. C.; Anderegg, J.; Porter, M. D. *Langmuir* **1998**, *15*, 518−525.
(75) Camon, K. T.; Hurley, L. G. *J. Phys. Chem.* **1991**, *95*, 9979−9984.
(76) Duan, L.; Garrett, S. J. *J. Phys. Chem. B* **2001**, *105*, 9812−9816.
(77) Heister, K.; Rong, H.-T.; Buck, M.; Zharnikov, M.; Grunze, M.; Johansson, L. S. O. *J. Phys. Chem. B* **2001**, *105*, 6888−6894.
(78) Rong, H.-T.; Frey, S.; Yang, Y.-J.; Zharnikov, M.; Buck, M.; Wuhn, M.; Woll, Ch.; Helmchen, G. *Langmuir* **2001**, *17*, 1582−1593.
(79) Weckenmann, U.; Mittler, S.; Naumann, K.; Fischer, R. A. *Langmuir* **2002**, *18*, 5479−5486.
(80) Gui, J. Y.; Stern, D. A.; Frank, D. G.; Lu, F.; Zapien, D. C.; Hubbard, A. T. *Langmuir* **1991**, *7*, 955−963.
(81) Gewirth, A. A.; Niece, B. K. *Chem. Rev.* **1997**, *97*, 1129−1162.
(82) Tamura, K.; Wang, J. X.; Adzic, R. R.; Ocko, B. M. *J. Phys. Chem. B* **2004**, *108*, 1992−1998.
(83) Leopold, M. C.; Black, J. A.; Bowden, E. F. *Langmuir* **2002**, *18*, 978−980.
(84) Chidsey, C. E. D.; Loiacono, D. N.; Nakahara, S.; Sleator, T. *Surf. Sci.* **1988**, *200*, 45−66.
(85) Burgess, J. D.; Hawkridge, F. M. *Langmuir* **1997**, *13*, 3781−3786.
(86) Wan, L.-J.; Terashima, M.; Noda, H.; Osawa, M. *J. Phys. Chem. B* **2000**, *104*, 3563−3569.
(87) Widrig, C. A.; Chung, C.; Porter, M. D. *J. Electroanal. Chem.* **1991**, *310*, 335−359.
(88) Bard, A. J.; Faulkner, L. R. *Electrochemical Methods, Fundamentals and Applications*, 2nd ed.; John Wiley & Sons: New York, 2001, p 167.
(89) Chen, C.-h.; Kepler, K. D.; Gewirth, A. A.; Ocko, B. M.; Wang, J. *J. Phys. Chem.* **1993**, *97*, 7290−1294.
(90) Li, X.; Gewirth, A. A. *J. Am. Chem. Soc.* **2003**, *125*, 7086−7099.
(91) Hagenstrom, H.; Esplandiu, M. J.; Kolb, D. M. *Langmuir* **2001**, *17*, 839−848.
(92) Chen, C.-h.; Gewirth, A. A. *J. Am. Chem. Soc.* **1992**, *114*, 5439−5440.
(93) Bain, C. D.; Troughton, E. B.; Tao, Y.-T.; Evall, J.; Whitesides, G. M.; Nuzzo, R. G. *J. Am. Chem. Soc.* **1989**, *111*, 321−335.
(94) Bain, C. D.; Whitesides, G. M. *J. Am. Chem. Soc.* **1989**, *111*, 7164−7175.
(95) Snyder, R. G. *J. Mol. Spectrosc.* **1961**, *7*, 116−144.
(96) Porter, M. D.; Bright, T. B.; Allara, D. L.; Chidsey, C. E. D. *J. Am. Chem. Soc.* **1987**, *109*, 3559−3568.
(97) Nuzzo, R. G.; Dubois, L. H.; Allara, D. L. *J. Am. Chem. Soc.* **1990**, *112*, 558−569.
(98) Walczak, M. M.; Chung, C.; Stole, S. M.; Widrig, C. A.; Porter, M. D. *J. Am. Chem. Soc.* **1991**, *113*, 2370−2378.
(99) Laibinis, P. E.; Whitesides, G. M.; Allara, D. L.; Tao, Y.-T.; Parikh, A. N.; Nuzzo, R. G. *J. Am. Chem. Soc.* **1991**, *113*, 7152−7167.
(100) Li, J.; Abruna, H. D. *J. Phys. Chem. B* **1997**, *101*, 244−252.
(101) Tillman, N.; Ulman, A.; Schildkraut, J. S.; Penner, T. L. *J. Am. Chem. Soc.* **1988**, *110*, 6136−6144.
(102) Bryant, M. A.; Pemberton, J. E. *J. Am. Chem. Soc.* **1991**, *112*, 8284−8293.
(103) Haehner, G.; Woell, C.; Buck, M.; Grunze, M. *Langmuir* **1993**, *9*, 1955−1958.
(104) Bryant, M. A.; Pemberton, J. E. *J. Am. Chem. Soc.* **1991**, *113*, 3629−3637.
(105) Chabal, Y. J. *Surf. Sci. Rep.* **1988**, *8*, 211−357.
(106) Zhong, C.-J.; Porter, M. D. *J. Am. Chem. Soc.* **1994**, *116*, 11616−11617.